Check for updates

JGR Oceans

RESEARCH ARTICLE
10.1029/2023JC019687

A Comparison of Arctic Ocean Sea Ice Export Between Nares Strait and the Canadian Arctic Archipelago

S. E. L. Howell[1], D. G. Babb[2], J. C. Landy[3], G. W. K. Moore[4,5], B. Montpetit[1], and M. Brady[1]

[1]Climate Research Division, Environment and Climate Change Canada, Toronto, ON, Canada, [2]Centre for Earth Observation Science, University of Manitoba, Winnipeg, MB, Canada, [3]Department of Physics and Technology, The Arctic University of Norway, Tromsø, Norway, [4]Department of Physics, University of Toronto, Toronto, ON, Canada, [5]Department of Chemical and Physical Sciences, University of Toronto Mississauga, Mississauga, ON, Canada

Key Points:

- First comparison of Arctic Ocean ice export between Nares Strait and the CAA
- No occurrence of large Arctic Ocean ice export events coinciding across all regions was observed
- Seasonal Arctic Ocean ice volume export from Nares Strait and the CAA together represent ~25% of the volume export from Fram Strait

Correspondence to:

S. E. L. Howell,
Stephen.Howell@ec.gc.ca

Citation:

Howell, S. E. L., Babb, D. G., Landy, J. C., Moore, G. W. K., Montpetit, B., & Brady, M. (2023). A comparison of Arctic Ocean sea ice export between Nares Strait and the Canadian Arctic Archipelago. *Journal of Geophysical Research: Oceans*, *128*, e2023JC019687. https://doi.org/10.1029/2023JC019687

Received 25 JAN 2023
Accepted 10 APR 2023

© 2023 His Majesty the King in Right of Canada and The Authors. Reproduced with the permission of the Minister of Environment and Climate Change. This is an open access article under the terms of the Creative Commons Attribution-NonCommercial-NoDerivs License, which permits use and distribution in any medium, provided the original work is properly cited, the use is non-commercial and no modifications or adaptations are made.

Abstract Nares Strait and the channels of the Canadian Arctic Archipelago (CAA) act as conduits for sea ice export from the Arctic Ocean but have never been directly compared. Here, we perform such a comparison for both the sea ice area and volume fluxes from October 2016 to December 2021. Nares Strait provided the largest average seasonal (October through September) ice area flux of $95 \pm 8 \times 10^3$ km^2 followed by the CAA regions of the Queen Elizabeth Islands (QEI) at $41 \pm 7 \times 10^3$ km^2 and M'Clure Strait at $2 \pm 8 \times 10^3$ km^2 with corresponding ice volume fluxes of 177 ± 15 km^3, 59 ± 10 km^3, and 8 ± 8 km^3, respectively. Larger Arctic Ocean ice export at Nares Strait was associated with a shorter ice arch duration (237 days) compared to M'Clure Strait (163 days) and QEI (65 days). Seasonal Arctic Ocean ice export was dominated by Nares Strait in 2017–2019 and 2021 but was remarkably exceeded by the QEI in 2020. Large-scale atmospheric circulation patterns were found to influence the ice area flux in the absence of ice arches but no occurrence of coherent Arctic Ocean ice export events coinciding across all gates were observed. Average net seasonal Arctic Ocean ice area and volume export were 138×10^3 km^2 and 245 km^3, which represent ~16% of the area and ~25% of the volume of sea ice export from Fram Strait. Divergent Arctic Ocean export ice trajectories are apparent for Nares Strait and the QEI when compared to Fram Strait.

Plain Language Summary Sea ice is transported out of the Arctic Ocean via Nares Strait and the channels of the Canadian Arctic Archipelago (CAA) but these export passageways have never been directly compared. Here, we perform such a comparison for both the sea ice area and volume fluxes from October 2016 to December 2021. Nares Strait provided the largest average seasonal fluxes followed by the CAA regions of the Queen Elizabeth Islands (QEI) and M'Clure Strait. Larger Arctic Ocean ice export at Nares Strait was associated less frequent ice arch formation that halts ice export compared to M'Clure Strait and QEI. No occurrence of a large Arctic Ocean ice export event coinciding across all regions was observed. Arctic Ocean ice export was dominated by Nares Strait in 2017–2019 and 2021 but was remarkably exceeded by the QEI in 2020. Under continued warming, Arctic Ocean ice export from Nares Strait and the QEI are expected to increase.

1. Introduction

The recent decline in the Arctic Ocean sea ice extent during the summer months (e.g., Parkinson & DiGirolamo, 2021) is one of the most visible features of a warmer Arctic. However, identifying the processes responsible for the Arctic's sea ice decline is challenging because ice is very dynamic and does not always melt locally. While a considerable amount of sea ice does melt locally in the Arctic Ocean (Babb et al., 2022; Kwok & Cunningham, 2010; Perovich et al., 2008), a large amount is also transported out of the Arctic Ocean to southern latitudes where it melts and delivers a considerable volume of freshwater to the global ocean (Kwok, 2004, 2009). The major passageways for southward Arctic Ocean ice export are Fram Strait, Nares Strait, the channels within the Canadian Arctic Archipelago (CAA), and the Bering Strait. There is inter-annual variability in Arctic Ocean ice export at these passageways but in general Fram Strait has historically provided the largest contribution with an average area ice export of 880×10^3 km^2 (Smedsrud et al., 2017). Arctic Ocean ice area export through Nares Strait and the CAA have been an order of magnitude lower than Fram Strait over the satellite observation era, with respective annual means between 42X10^3 km^2 and 87 $\times$ 10 km^2 (Kwok et al., 2010; Moore et al., 2021) and 25×10^3 km^2 (Howell & Brady, 2019), respectively. Finally, sea ice export through the Bering Strait has not

21699291, 2023, 4, Downloaded from https://agupubs.onlinelibrary.wiley.com/doi/10.1029/2023JC019687 by Arctic University of Norway - UIT Tromso, Wiley Online Library on [17/07/2023]. See the Terms and Conditions (https://onlinelibrary.wiley.com/terms-and-conditions) on Wiley Online Library for rules of use; OA articles are governed by the applicable Creative Commons License

Table 1
SAR Image Products Used in This Analysis

Platform	Beam mode	Pixel spacing (m)	Swath (km)
RADARSAT-2	ScanSAR Wide (SCWA-SGF)	50	500
RCM	ScanSAR Medium Resolution (SC30 M)	30	125
RCM	ScanSAR Medium Resolution (SC50 M)	50	350
RCM	ScanSAR Low Resolution (SC100 M)	100	500
RCM	ScanSAR Low Noise (SCLN)	100	350
Sentinel-1	Extra-Wide Swath – Medium (EW-GRDM)	40	410

been explicitly quantified, but can occur episodically and is assumed to be quite small compared to the other gates (Babb et al., 2013).

There is a growing body of evidence that the Arctic Ocean ice export contributions from Nares Strait and the CAA are increasing as a result of climate change. Recently, it has been demonstrated that the ice arches in Nares Strait and the ice arches that ring the CAA have deteriorated over the past 20+ years leading to a corresponding increase in Arctic Ocean ice export (Howell & Brady, 2019; Moore et al., 2021). Increased Arctic Ocean ice export through Nares Strait and the CAA have widespread downstream implications. For example, the presence of an ice arch in Nares Strait contributes to the formation of the North Water Polynya (NOW), which is a region of considerable biological activity (Barber et al., 2001; Melling et al., 2001). Increased Arctic Ocean ice export through the CAA poses hazardous conditions for ships transiting through the Northwest Passage (Haas & Howell, 2015; Howell, Babb, et al., 2022; Melling, 2002). Ice export via Nares Strait and the CAA can reach as far as the East Coast of Newfoundland, causing hazardous ice conditions (Barber et al., 2018). Increased Arctic Ocean export also reduces the reservoir of the oldest and thickest ice in the Arctic that is located to the north of the CAA and Greenland (Landy et al., 2022; Maslanik et al., 2011; Melling, 2002; Moore et al., 2019; Ryan & Münchow, 2017; Tilling et al., 2015). This region has been termed The Last Ice Area as it is expected to be the last region in the Arctic to contain sea ice during the summer months and as a result, is expected to be the last refuge for marine dependent species (Durner et al., 2009; Hamilton et al., 2014; Newton et al., 2021).

Considering the importance of Arctic Ocean ice export via Nares Strait and the CAA, it is necessary to understand their relative contributions with respect to total Arctic Ocean ice export. Here, we use the latest satellite observations of sea ice to directly compare the ice area and volume fluxes from the Arctic Ocean to Nares Strait and the CAA from October 2016 to December 2021, encompassing 5 ice seasons. We evaluate the net seasonal ice fluxes and their variations between regions in the context of forcing by large-scale atmospheric circulation and regional ice conditions.

2. Data

The primary data used in this analysis was C-band synthetic aperture radar (SAR) imagery at HH polarization from RADARSAT-2 (2016–2020), Sentinel-1 (2016–2021), and the RADARSAT Constellation Mission (RCM) (2020–2012) (Table 1). Although sea ice motion can be detected using HV polarization (e.g., Komarov & Barber, 2014), we selected HH polarization because more HH imagery is available in the early part of the record and our aim was to create a consistent time series. Moreover, previous studies have typically just utilized HH polarization in these regions (e.g., Howell & Brady, 2019; Kwok, 2006; Kwok et al., 2010). Sentinel-1 imagery is available at the Copernicus Open Access Hub (https://scihub.copernicus.eu/dhus/#/home). The RADARSAT-2 and RCM imagery is available online at Natural Resources Canada's Earth Observation Data Management System (https://www.eodms-sgdot.nrcan-rncan.gc.ca). All SAR images were resampled to a spatial resolution of 200 m. Using all available SAR imagery from all sensors from October 2016 to December 2021, the average temporal sample window over Nares Strait and the CAA was ~1 day.

We also make use of year-round sea ice thickness (SIT) estimates obtained from the CryoSat-2 radar altimeter (Landy et al., 2022) updated to cover our study period from October 2016 to July 2021. Note, SIT measurements are unavailable from August–December 2021. This record combines sea ice freeboard measurements obtained during the "cold" season between October and April, using the method described in Landy et al. (2020), and

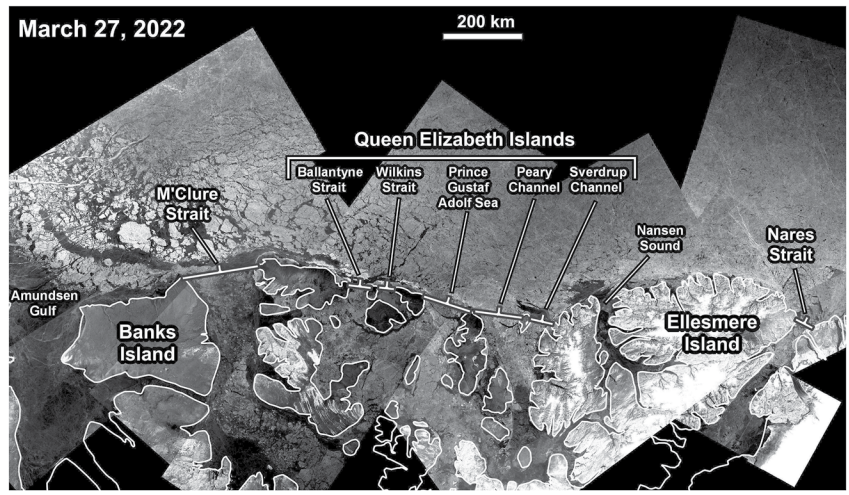

Figure 1. Map of the Canadian Arctic with the location of the Arctic Ocean sea ice flux gates used in this study. Background is RADARSAT Constellation Mission (RCM) imagery on 27 March 2022. (RCM © Government of Canada).

during the summer between May and September using the method described in Dawson et al. (2022). A bias correction based on radar model simulations, as described in Landy et al. (2022), is applied to the summer freeboards, before the freeboards are converted to a continuous pan-Arctic record of SIT using snow loading information from the Lagrangian snow evolution scheme SnowModel-LG (Stroeve et al., 2020). Year-round SIT observations from CryoSat-2 are available from https://data.bas.ac.uk/full-record.php?id=GB/NERC/BAS/PDC/01613.

Additional supporting data used in this analysis include weekly total and multi-year ice (MYI) concentration from the Canadian Ice Service (CIS) digital ice charts (Tivy et al., 2011) available at https://iceweb1.cis.ec.gc.ca/Archive/page1.xhtml?lang=en, weekly large-scale RCM and Sentinel-1 sea ice motion data (Howell, Brady, & Komarov, 2022) available at https://open.canada.ca/data/en/dataset/22aa3b41-425f-4f67-9747-f097c00e3eb1 and monthly sea level pressure (SLP) and 10 m wind speed from ERA5 (Copernicus Climate Change Service (C3S), 2017) available at https://cds.climate.copernicus.eu/cdsapp#!/home.

3. Methods

The Arctic Ocean sea ice area flux between the Nares Strait and CAA was estimated monthly from October 2016 to December 2021. The Nares Strait flux gate is located between Ellesmere Island and Greenland with a 139 km aperture (Figure 1), this gate was also used in Moore et al. (2021). The CAA flux gates consist of M'Clure Strait and the Queen Elizabeth Islands (QEI) which collectively are made of Ballantyne Strait, Wilkins Strait, Prince Gustaf Adolf Sea, Peary Channel, and Sverdrup Channel (Figure 1) that have been used in previous studies (e.g., Howell & Brady, 2019; Howell, Wohlleben, Dabboor, et al., 2013). M'Clure Strait has an aperture of 183 km and the total aperture of all QEI gates is 370 km. For this analysis we do not consider the Arctic Ocean sea ice area flux at Amundsen Gulf because (a) the region typically only experiences Arctic Ocean ice import (Agnew et al., 2008; Kwok, 2006), (b) virtually no MYI is found in the region, and (c) the region always becomes ice-free in the summer months (CIS, 2021). We also do not consider the Arctic Ocean sea ice area flux at Nansen Sound because of its small aperture together with the small channels that limit the magnitude of southward ice transport into the CAA (Figure 1). In addition, there is an ice plug (barrier) that forms at the mouth of Nansen Sound (Serson, 1972) which is known to have until recently not broken up for decades (Alt et al., 2006; Jeffers et al., 2001; Melling, 2002) and during our study period it did not break up in 2017, 2018, and 2021.

We use a widely established methodology to estimate the sea ice area flux at the aforementioned gates (Agnew et al., 2008; Howell & Brady, 2019; Howell, Wohlleben, Dabboor, et al., 2013; Kwok, 2006; Kwok et al., 2010; Moore et al., 2021). For each SAR image pair, sea ice motion was estimated using the Environment and Climate Change Canada Automated Sea Ice Tracking System (ECCC-ASITS; Howell, Brady, & Komarov, 2022) that is based on the Komarov and Barber (2014) feature tracking algorithm. The resulting sea ice motion estimates are

21699291, 2023, 4, Downloaded from https://agupubs.onlinelibrary.wiley.com/doi/10.1029/2023JC019687 by Arctic University of Norway - UIT Tromso, Wiley Online Library on [17/07/2023]. See the Terms and Conditions (https://onlinelibrary.wiley.com/terms-and-conditions) on Wiley Online Library for rules of use; OA articles are governed by the applicable Creative Commons License

21699291, 2023, 4, Downloaded from https://agupubs.onlinelibrary.wiley.com/doi/10.1029/2023JC019687 by Arctic University of Norway - UIT Tromso, Wiley Online Library on [17/07/2023]. See the Terms and Conditions (https://onlinelibrary.wiley.com/terms-and-conditions) on Wiley Online Library for rules of use; OA articles are governed by the applicable Creative Commons License

interpolated using inverse distance weighting to each gate with a 30 km buffer on either side and then sampled at 5 km internals across each gate. The sea ice area flux (F) was calculated using the following equation:

$$\mathbf{F} = \sum \mathbf{c_i u_i}\, \Delta \mathbf{x} \tag{1}$$

where, Δx is the spacing along each gate (i.e., 5 km), u_i is the ice motion normal to the flux gate at the ith location and c_i is the sea ice concentration determined from the CIS ice charts. Positive flux values represent Arctic Ocean ice export (i.e., Arctic Ocean ice export into Nares Strait and/or the CAA) and negative flux values represent Arctic Ocean ice import (i.e., ice import into the Arctic Ocean from Nares Strait and/or the CAA). For all gates, the sea ice area flux values were summed over each month from October 2016 to December 2021. The corresponding sea ice volume flux from October 2016 to July 2021 was then determined from the product of the monthly ice area flux and the monthly average CryoSat-2 ice thickness value within the 30 km buffer around each gate.

The uncertainty (σ_f) in F can be estimated following Kwok and Rothrock (1999) by assuming errors in sea ice motion are additive, uncorrelated, and normally distributed using the following equation:

$$\boldsymbol{\sigma_f} = \frac{\boldsymbol{\sigma_e L}}{\sqrt{\mathbf{N_s}}} \tag{2}$$

where, σ_e is the error in SAR derived ice motion, L is the width of the gate, and N_s is the number of samples across the gate. Komarov and Barber (2014) estimated the feature tracking algorithm used by the ECCC-ASITS has an σ_e of 0.43 km based on buoy comparison in the Beaufort Sea during the winter. Howell, Brady, and Komarov (2022) considered all Arctic buoys above 40°N without removing any outliers or imposing any quality flags on the buoys (e.g., Lindsay & Stern, 2003) and reported an σ_e of 2.78 km for the winter (dry) months and an σ_e of 3.43 km for the summer (wet) months. Solving Equation 2 with this range of σ_e values indicates that σ_f over the sampling interval ranges from 12 to 92 km^2 at Nares Strait, 13–103 km^2 at M'Clure Strait, and 18–148 km^2 at the QEI. We expect the σ_f at the gates in this study to be closer to their lower bounds given that there is typically high sea ice concentration at these flux gates even during the summer months (CIS, 2021) which facilitates more robust feature detection compared to the marginal ice zone (e.g., Kwok et al., 1998).

4. Results and Discussion

4.1. Monthly and Seasonal Ice Flux Comparison

The monthly time series of ice area flux at Nares Strait, the QEI, and M'Clure Strait for October 2016 to December 2021 is shown in Figure 2. Over the time period, Nares Strait and the QEI primarily experienced Arctic Ocean ice export, whereas M'Clure Strait experienced both Arctic Ocean ice import and export but ice export occurred more frequently (Figure 2). Arctic Ocean ice export at Nares Strait and the QEI was primarily MYI whereas the ice crossing M'Clure Strait was a more of a mix of seasonal and MYI ice (Figure 2). For Nares Strait, the monthly sea ice area flux ranged from 40×10^3 km^2 (October 2017) to 2×10^3 km^2 (August 2019) (Figure 2a). The sea ice area flux at the QEI gates ranged from 49×10^3 km^2 (September 2020) to -12×10^3 km^2 (August 2019) with September 2020 at QEI exhibiting the largest monthly ice flux of all the gates considered (Figure 2b). The ice area flux at M'Clure Strait ranged from to 28×10^3 km^2 (August 2021) to -47×10^3 km^2 (October 2021), with the latter being the largest Arctic Ocean ice import value for all gates over the time period (Figure 2c).

The monthly time series of ice volume flux at Nares Strait, the QEI, and M'Clure Strait from October 2016 to July 2021 is shown in Figure 3. The largest monthly volume flux of 68 km^3 (May 2017) occurred at Nares Strait followed by 54 km^3 (September 2020) at the QEI (Figure 3ab). The largest volume flux at M'Clure Strait was -28 km^3 (January 2021) indicating Arctic Ocean ice import whereas the largest Arctic Ocean ice export at M'Clure Strait was 16 km^3 (September 2018) (Figure 3c). The interannual variability of the ice volume flux was similar to the ice area flux at all gates but there are some notable differences. For instance, the ice area flux values in Nares Strait were clearly lower during 2019 than in 2017 however, the volume fluxes were not as low between 2019 and 2017 (Figures 2a and 3a). This reflects the importance of the SIT variability in controlling total ice volume fluxes as the ice area flux is not always the dominant driver of the volume flux variability. Also, the sea ice volume flux has been noticeably lower since 2020 for Nares Strait (Figure 3a). Ryan and Münchow (2017)

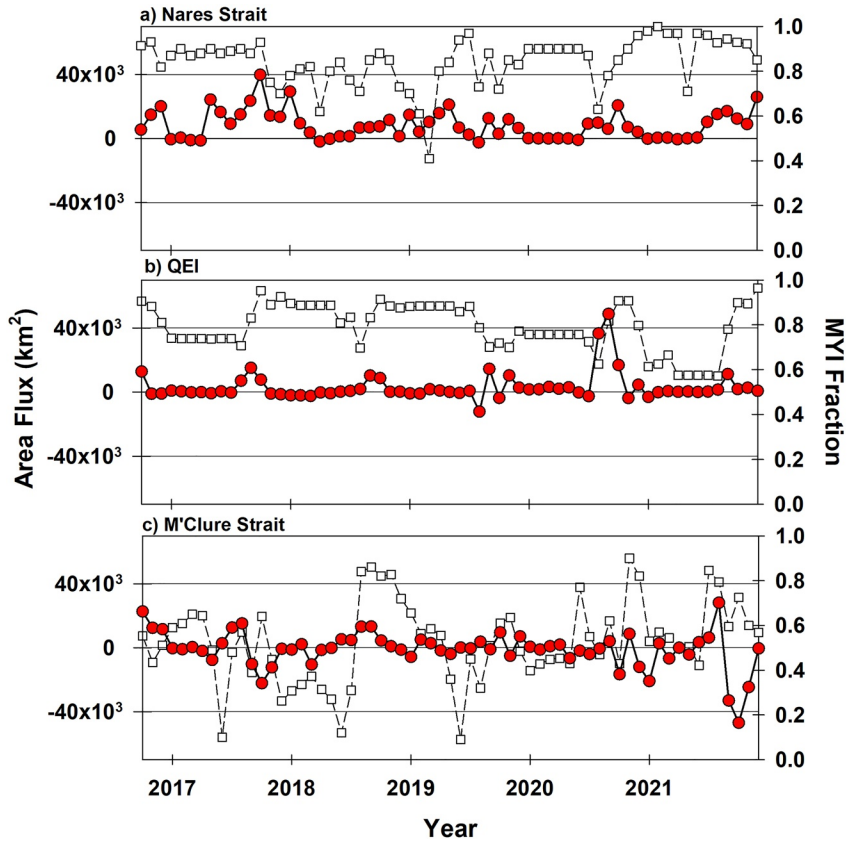

Figure 2. Time series of Arctic Ocean sea ice area flux (solid red circles) and multi-year ice concentration (squares) at (a) Nares Strait, (b) Queen Elizabeth Islands (QEI), and (c) M'Clure Strait from October 2016 to December 2021. Positive flux values are southward sea ice export, and negative values are northward sea ice import.

reported no thinning trend for ice in Nares Strait from 2003 to 2012 as observed by in situ upward looking sonars, however, Moore et al. (2021) reported thinning ice in the Lincoln Sea north of Nares Strait using Pan-Arctic Ice Ocean Modeling and Assimilation System (PIOMAS, Zhang & Rothrock, 2003) data from 1997 to 2019. Our volume flux estimates use CryoSat-2 ice thickness values and reflect the thinner trend noted by Moore et al. (2021).

The seasonal (October to September) ice area and volume flux for the 2017 to 2021 ice seasons are shown Figure 4. Over these 5 years, the average seasonal ice area flux was $95 \pm 8 \times 10^3$ km^2 for Nares Strait, $41 \pm 7 \times 10^3$ km^2 for the QEI, and $2 \pm 8 \times 10^3$ km^2 for M'Clure Strait (Figure 4a). The corresponding average seasonal ice volume fluxes for the Nares Strait, the QEI, and M'Clure Strait were 177 ± 15 km^3, 59 ± 10 km^3, and 8 ± 8 km^3, respectively (Figure 4b). On average, Arctic Ocean ice export via Nares Strait was ~2 times larger for the area flux and ~3 times larger for volume flux than it was for the QEI.

From 2017 to 2021, the net ice area flux of all three gates ranged from 58×10^3 km^2 (2021) to 216×10^3 km^2 (2017) (Figure 4a) and the volume flux ranged from 174 km^3 (2020) to 327 km^3 (2017) (Figure 4b). The average net ice area flux of all three gates was 138×10^3 km^2, which represents 16% of the Arctic Ocean ice export through Fram Strait based on the seasonal value of 880×10^3 km^2 reported by Smedsrud et al. (2017). The average net volume flux was 245 km^3 and represents 25% of the recent 2010 to 2018 average volume flux from Fram Strait (Sumata et al., 2022). Specifically for 2018, the volume flux from Nares Strait and the CAA represents 32% of the 590 km^3 Fram Strait volume flux reported by Sumata et al. (2022). It seems apparent that over the long-term record, the seasonal ice volume flux at Fram Strait (Spreen et al., 2020; Sumata et al., 2022) and at Nares Strait and the CAA (Howell & Brady, 2019; Kwok et al., 2010; Moore et al., 2021, Figure 4b) are following divergent trajectories. Figure 4 also points out that Nares Strait and the QEI make-up the dominant ice area and volume flux contributions but the oscillating nature of the ice flux at M'Clure Strait does influence the net seasonal flux,

21699291, 2023, 4, Downloaded from https://agupubs.onlinelibrary.wiley.com/doi/10.1029/2023JC019687 by Arctic University of Norway - UIT Tromso, Wiley Online Library on [17/07/2023]. See the Terms and Conditions (https://onlinelibrary.wiley.com/terms-and-conditions) on Wiley Online Library for rules of use; OA articles are governed by the applicable Creative Commons License

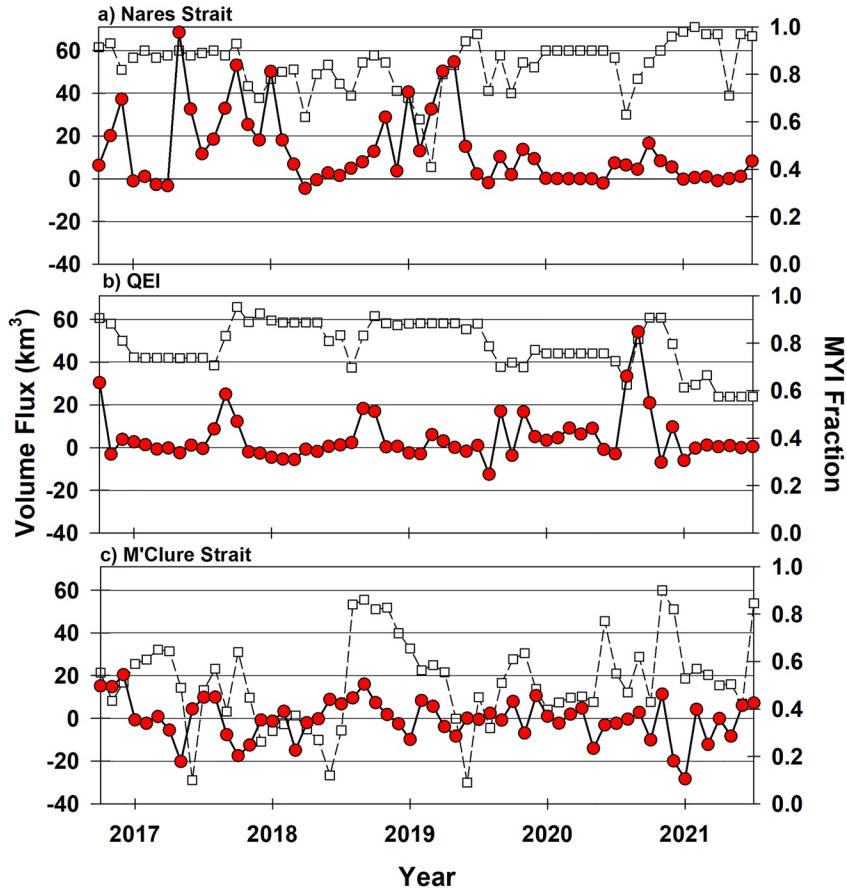

Figure 3. Time series of Arctic Ocean sea ice volume flux (solid red circles) and multi-year ice concentration (squares) at (a) Nares Strait, (b) Queen Elizabeth Islands (QEI), and (c) M'Clure Strait from October 2016 to July 2021. Positive flux values are southward sea ice export, and negative values are northward sea ice import.

with years of Arctic Ocean ice import through M'Clure Strait offsetting Arctic Ocean ice export through the QEI and Nares. For example, 2021 would have experienced a much higher net seasonal ice area flux if it were not for the -45×10^3 km^2 of Arctic Ocean ice import at M'Clure Strait (Figure 4a).

A striking feature to note from Figure 4 is that from 2017 to 2019 and again in 2021 Nares Strait was the primary Arctic Ocean ice export passageway but in 2020 the QEI was the dominate passageway with ice area flux of 120×10^3 km^2 and volume flux of 134 km^3. While it is generally assumed that Nares Strait contributes the second largest amount of Arctic Ocean ice export on a seasonal basis relative to Fram Strait (e.g., Kwok et al., 2010; Moore et al., 2021), Figure 4 provides evidence that Arctic Ocean ice export via the QEI can exceed Nares Strait.

4.2. Ice Arch Formation and Sea Ice Area Flux Variability

Boxplots of monthly sea ice area flux values at Nares Strait, the QEI and M'Clure Strait are shown in Figure 5. The most notable feature of monthly variability between all regions is that the ice area flux declined considerably between December and July at M'Clure Strait and the QEI whereas, Nares Strait experienced appreciable ice area flux in all months (Figure 5). We attribute the reduced ice area fluxes in the regions of the CAA to ice arches that limit ice movement (CIS, 2021; Hibler et al., 2006; Melling, 2002). For Nares Strait, the ice arch that forms between Ellesmere Island and Greenland also stops the ice flux between the Arctic Ocean and Nares Strait (Kwok, 2005). However, there is considerable variability in the formation and collapse of the Nares Strait arch (Kirillov et al., 2021; Kwok et al., 2010; Moore et al., 2021; Vincent, 2019) that in turn results in more monthly ice flux variability, compared to the relatively consistent ice arches forming across CAA gates.

The enhanced variability is evident when looking at the timing of ice arch collapse, formation, and annual ice flux duration in Nares Strait, the QEI and M'Clure Strait from 2017 to 2021, which are identified in Table 2,

21699291, 2023, 4, Downloaded from https://agupubs.onlinelibrary.wiley.com/doi/10.1029/2023JC019687 by Arctic University of Norway - UIT Tromso, Wiley Online Library on [17/07/2023]. See the Terms and Conditions (https://onlinelibrary.wiley.com/terms-and-conditions) on Wiley Online Library for rules of use; OA articles are governed by the applicable Creative Commons License

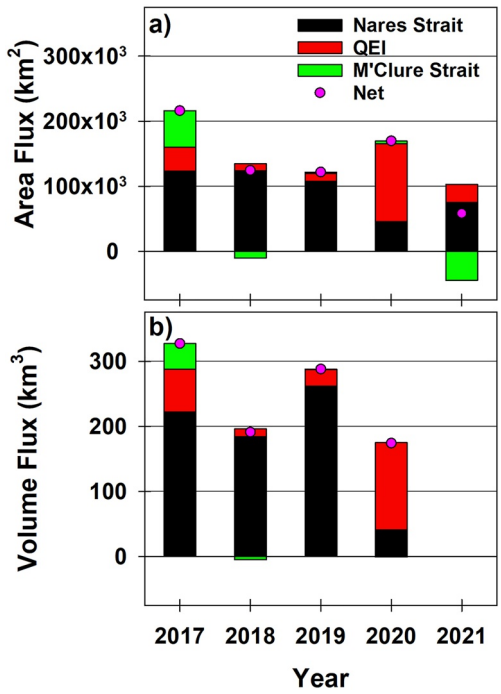

Figure 4. Seasonal (October to September) ice (a) area and (b) volume flux through Nares Strait, the Queen Elizabeth Islands (QEI), and M'Clure Strait for 2017 to 2021. Positive flux values are southward sea ice export, and negative values are northward sea ice import. Note the seasonal volume flux was not available for 2021.

Table 3, and Table 4, respectively. On average, the October to September ice flux duration (i.e., absence of an ice arch) in Nares Strait was 237 ± 77 days, followed by 163 ± 21 days in M'Clure Strait, and 65 ± 29 days in the QEI (Tables 2–4). There was less variability in timing of ice arch formation within the QEI and M'Clure Strait compared to Nares Strait but it is important to highlight that for the years under consideration, Nares Strait ice arches exhibited anomalous behavior as evident with the early arch collapse in May 2017 (Moore & McNeil, 2018) and no arch formed in 2019 (Moore et al., 2021, Table 2). Though these recent events are anomalous compared to the historical record of the ice arches, they are expected to become more common with continued Arctic warming.

4.3. Forcing by Large-Scale Atmospheric Circulation and Regional Ice Conditions

Sea ice motion is primarily influenced by wind and moves parallel to sea level pressure (SLP) isobars (Thorndike & Colony, 1982). When ice arches are not present, SLP is known to influence the magnitude and direction ice flux between the Arctic Ocean and Nares Strait and the CAA (Agnew et al., 2008; Howell, Wohlleben, Dabboor, et al., 2013; Kwok, 2006; Moore & McNeil, 2018; Samelson et al., 2006). The net seasonal ice area flux at the gates indicates the general contribution to Arctic Ocean ice import or export (Figure 5) however, there are sizable monthly anomalies in the time series at all gates (Figure 2) that indicate short 1–2 months episodes of extreme ice motion can be sufficiently large in magnitude to dominate the net flux for the entire annual ice season. Moreover, an interesting feature of Figure 2 is there are no months where large Arctic Ocean ice export or import occurred coincidently across all gates. The correlation coefficients between monthly fluxes across all gates were only between −0.2 and 0.14. Next, we use the month of each gate's largest ice area flux to discuss the influence of atmospheric circulation and ice conditions coincident across all gates.

4.3.1. Nares Strait: October 2017

From October 2016 to December 2021, the largest monthly sea ice area flux in Nares Strait was 40×10^3 km^2 that occurred during October 2017. This single month value was almost equivalent to the 1997–2009 seasonal average of 42×10^3 km^2 reported by Kwok et al. (2010) and represented just less than half of the 2017–2019 seasonal average of 86×10^3 km^2 reported by Moore et al. (2021). Figure 6 illustrates how considerable Arctic Ocean ice was funneled through Nares Strait during October of 2017. Atmospheric circulation during October 2017 was characterized by a more intense Beaufort High that was shifted eastwards from its climatological location resulting in an eastward displacement of the anti-cyclonic circulation associated with the Beaufort High (Figure 7a). As a result, southerly winds were present over the Lincoln Sea just north of Nares Strait and drove sea ice toward Nares Strait (Figure 7d). The ice arch in Nares Strait had collapsed 5 months earlier, in May and open water in Baffin Bay (i.e., an absence of buttressing by sea ice) was available to accommodate Arctic Ocean ice export (Figure 8a; Table 2).

While the October SLP pattern and ice conditions were able to facilitate considerable Arctic Ocean ice export at Nares Strait, the ice area fluxes were markedly different at the QEI and M'Clure Strait with values of 8×10^3 km^2 and -22×10^3 km^2, respectively. This indicates the QEI received 80% less Arctic Ocean ice export compared to Nares Strait and M'Clure Strait contributed to Arctic Ocean ice import. Ice conditions in the CAA on 17 October 2017 indicated no ice arch in M'Clure Strait (Figure 8a; Table 4) but the ice arches had formed at all the gates within the QEI with the exception of the middle gate (Prince Gustaf Adolf Sea) (Figure 8a; Table 3). The October 2017 atmospheric conditions, most notably the shift in the Beaufort Gyre, facilitated Arctic Ocean ice import from M'Clure Strait and could have potentially facilitated considerable ice export through the QEI gates but ice arches limited the export to a single channel at the QEI. Moreover, there was high sea ice concentration throughout the majority of the CAA in October 2017, including in the Prince Gustaf Adolf Sea, which acted as a

21699291, 2023, 4, Downloaded from https://agupubs.onlinelibrary.wiley.com/doi/10.1029/2023JC019687 by Arctic University of Norway - UIT Tromso, Wiley Online Library on [17/07/2023]. See the Terms and Conditions (https://onlinelibrary.wiley.com/terms-and-conditions) on Wiley Online Library for rules of use; OA articles are governed by the applicable Creative Commons License

21699291, 2023, 4, Downloaded from https://agupubs.onlinelibrary.wiley.com/doi/10.1029/2023JC019687 by Arctic University of Norway - UIT Tromso, Wiley Online Library on [17/07/2023]. See the Terms and Conditions (https://onlinelibrary.wiley.com/terms-and-conditions) on Wiley Online Library for rules of use; OA articles are governed by the applicable Creative Commons License

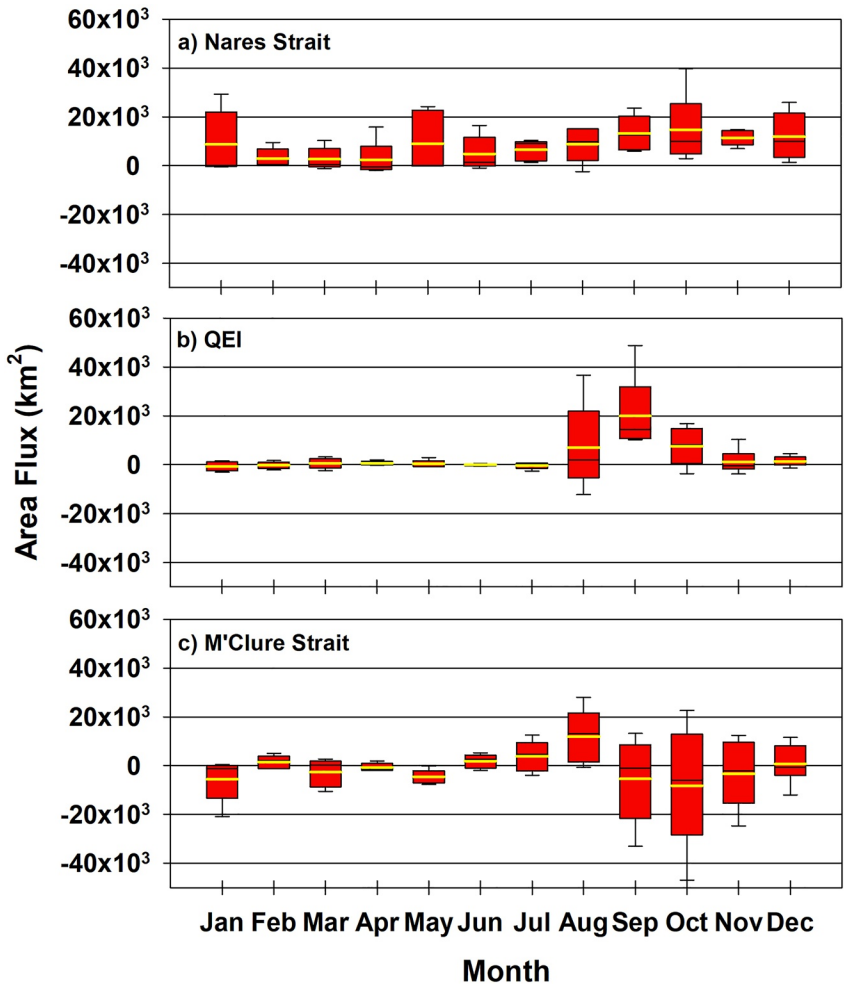

Figure 5. Box plots of mean monthly sea ice area flux from January to December at (a) Nares Strait, (b) Queen Elizabeth Islands (QEI), and (c) M'Clure Strait. The yellow line in the boxes indicates the mean.

buttress limiting the open water available to accommodate new ice imported from the Arctic Ocean (Figure 8a). Large-scale atmospheric circulation patterns certainly drives the ice area flux across all the gates and may force ice motion in the same direction at several gates, but locally different ice arch and buttressing conditions can still contribute to significant regional ice flux variability.

Table 2
Date of Ice Arch Formation, Collapse, and Season Ice Flux Duration (October to September) in Nares Strait for the 2017 to 2021 Seasons

Year	Formation	Collapse	Seasonal flux duration (days)
2017	30 January 2017	15 May 2017	259
2018	5 March 2018	2 July 2018	245
2019	–	–	365
2020	23 December 2019	29 June 2020	176
2021	7 December 2020	19 July 2021	140

Note. "–" indicates no ice formation or collapse. The date of collapse and formation was estimated using data from the Canadian Ice Service weekly ice charts and therefore has an uncertainty of ±7 days.

4.3.2. QEI: September 2020

From October 2016 to December 2021, the largest monthly sea ice area flux at the QEI was 49×10^3 km^2 and occurred during September 2020. Figure 9 illustrates how considerable Arctic Ocean ice was transported through the Prince Gustaf Adolf Sea region of the QEI during September 2020. Remarkably, this was the largest monthly ice flux to occur at the QEI when compared to the long-term record of ice area flux for the region available since 1997 (Howell & Brady, 2019). The September 2020 ice area flux value for the QEI was also larger than any previous monthly value observed in Nares Strait from 1997 to 2009 (Kwok et al., 2010) and from 2016 to 2021 (Moore et al., 2021, Figure 2ab). Atmospheric circulation during September 2020 was characterized by a shift of the Beaufort High toward Siberia as well as an intrusion of low pressure associated with the Lofoten Low that was displaced north of Svalbard, creating a strong pressure gradient directly over the QEI and resulting in southerly flow (Figure 7b) and ice motion (Figure 7e) directly

21699291, 2023, 4, Downloaded from https://agupubs.onlinelibrary.wiley.com/doi/10.1029/2023JC019687 by Arctic University of Norway - UIT Tromso, Wiley Online Library on [17/07/2023]. See the Terms and Conditions (https://onlinelibrary.wiley.com/terms-and-conditions) on Wiley Online Library for rules of use; OA articles are governed by the applicable Creative Commons License

Table 3
Date of Ice Arch Formation, Collapse, and Season Ice Flux Duration (October to September) in the Queen Elizabeth Islands for the 2017 to 2021 Seasons

Year	Region	Formation	Collapse	Seasonal flux duration (days)
2017	***Ballantyne Strait***	5 December 2016	28 August 2017	98
2018		16 October 2017	–	15
2019		–	26 August 2019	35
2020		11 November 2019	10 August 2020	92
2021		14 December 2020	–	74
2017	***Wilkins Strait***	24 October 2016	–	23
2018		–	–	0
2019		–	26 August 2019	35
2020		14 October 2019	10 August 2020	55
2021		21 September 2020	–	0
2017	***Prince Gustaf Adolf Sea***	26 December 2016	21 August 2017	126
2018		30 October 2017	–	29
2019		19 November 2018	5 August 2019	105
2020		25 November 2019	3 August 2020	113
2021		21 December 2020	16 August 2021	126
2017	***Peary Strait***	28 November 2016	21 August 2017	98
2018		16 October 2017	20 August 2018	56
2019		26 November 2018	29 July 2019	119
2020		25 November 2019	3 August 2020	113
2021		30 November 2020	16 August 2021	105
2017	***Sverdrup Strait***	7 November 2016	–	37
2018		–	–	0
2019		–	19 August 2019	12
2020		25 November 2019	3 August 2020	83
2021		30 November 2020	16 August 2021	60

Note. "–" indicates no ice formation or collapse. The date of collapse and formation was estimated using data from the Canadian Ice Service weekly ice charts and therefore has an uncertainty of ±7 days.

toward this region. All ice arches within the QEI broke before September 2020 (Table 3) and ice concentrations on 14 September 2020 indicated considerable open water available to accommodate new sea ice area imported from the Arctic Ocean (Figure 8b).

Table 4
Date of Ice Arch Formation, Collapse, and Season Ice Flux Duration (October to September) in M'Clure Strait for the 2017 to 2021 Seasons

Year	Formation	Collapse	Seasonal flux duration (days)
2017	16 January 2017	17 July 2017	182
2018	18 December 2017	23 July 2018	147
2019	31 December 2018	22 July 2019	161
2020	9 December 2019	27 July 2020	134
2021	25 January 2021	19 July 2021	189

Note. "-" indicates no ice formation or collapse. The date of collapse and formation was estimated using data from the Canadian Ice Service weekly ice charts and therefore has an uncertainty of ±7 days.

The Nares Strait ice arch was absent during September 2020 (Figure 8b; Table 2) but the resulting Arctic Ocean ice flux was still only 6×10^3 km^2. At M'Clure Strait, the ice arch was also absent (Table 4; Figure 8b) but Arctic Ocean ice export was also small at 4×10^3 km^2. It is clear that the SLP gradients were ideally located to drive a large ice flux into the QEI but could only drive ice motion perpendicular to the Nares and M'Clure Straits producing much smaller ice fluxes. Indeed, there have been many years where the ice arches in the QEI broke even earlier than they did in 2020 but did not combine with a large-scale atmospheric circulation pattern to induce such a large Arctic Ocean ice export (e.g., Alt et al., 2006; Howell & Brady, 2019; Howell, Wohlleben, Komarov, et al., 2013). The fact that Arctic Ocean ice export via the QEI exceeded Nares Strait during the 2020 season was even more remarkable because the QEI typically has a much shorter time window for ice export to occur compared to Nares Strait (64 vs. 237 days with no ice

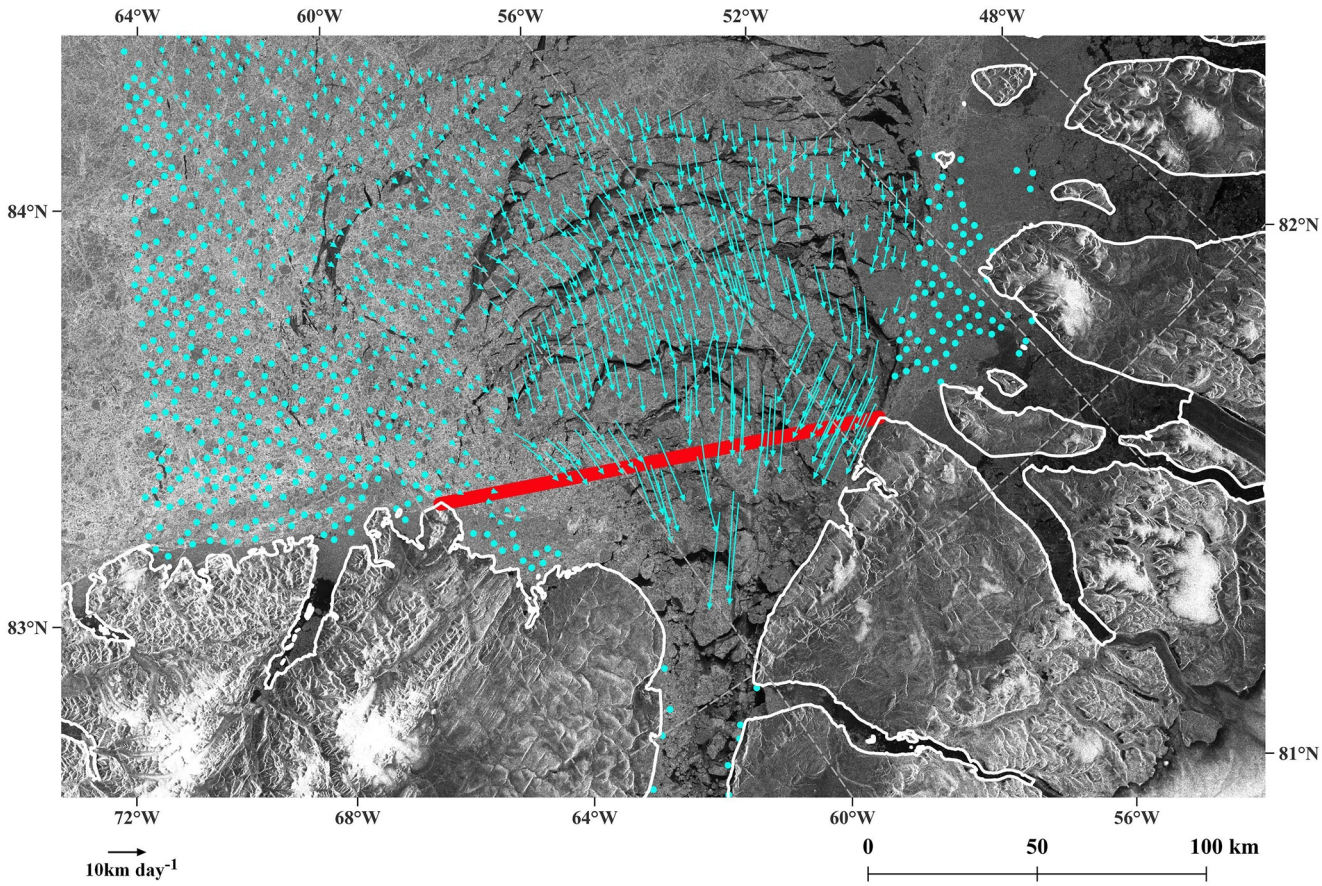

Figure 6. RADARSAT-2 derived sea ice motion vectors (km/day) between 11 October 2017 and 12 October 2017 over Nares Strait. The red line corresponds to the flux gate. Background is RADARSAT-2 image on 11 October 2017. RADARSAT-2 Data and Products © Macdonald Dettwiler, and Associates Ltd. (2017).

arch; Tables 2 and 3). Despite favorable ice conditions, the large Arctic Ocean ice export in September 2020 only via QEI underscores that the location of high and low SLP pressure regions across the Arctic is another important factor that contributes to the Arctic Ocean ice flux variability at these regions.

4.3.3. M'Clure Strait: October 2021

From October 2016 to December 2021, the sea ice area flux in October 2021 of -47×10^3 km^2 was the largest for M'Clure Strait. Figure 10 illustrates Arctic Ocean ice import during October 2021 at M'Clure Strait. Placing this in context of the historical record since 1997 indicates it was the second largest monthly Arctic Ocean ice import at this gate, and was only slightly less than the largest import of -51×10^3 km^2 which occurred in October 2007 (Howell & Brady, 2019). The atmospheric circulation during October 2021 was characterized by high pressure over the central Arctic resulting from an extreme eastward shift in the Beaufort High as well as low pressure over Alaska resulting in strong anti-cyclonic atmospheric flow (Figure 7c) and ice motion (Figure 7f) over the Beaufort Sea. No ice arch was present in M'Clure Strait during 18 October 2021 (Figure 8c; Table 4).

At Nares Strait the ice area flux was 12×10^3 km^2 and at the QEI it was 2×10^3 km^2. The SLP pattern during October 2021 was not conducive for Arctic Ocean ice export at the QEI (Figure 7c) despite no arches being present (Figure 8c; Table 3) but it was more favorable for Arctic Ocean ice export to Nares Strait (Figure 7c) where an ice arch was also not present (Figure 8c; Table 2). Again, the location of the corresponding high and low SLP centers of action across the Arctic play a significant role in the Arctic Ocean ice flux variability experienced across the three gates. The large swings in the ice flux time series for M'Clure Strait (Figure 2) indicate the region is more susceptible to large-scale atmospheric circulation variability compared to the QEI and Nares Strait, that we attribute to its relative proximity to the Beaufort High and typically lower sea ice concentrations reducing buttressing effects on ice at the gate.

21699291, 2023, 4, Downloaded from https://agupubs.onlinelibrary.wiley.com/doi/10.1029/2023JC019687 by Arctic University of Norway - UIT Tromso, Wiley Online Library on [17/07/2023]. See the Terms and Conditions (https://onlinelibrary.wiley.com/terms-and-conditions) on Wiley Online Library for rules of use; OA articles are governed by the applicable Creative Commons License

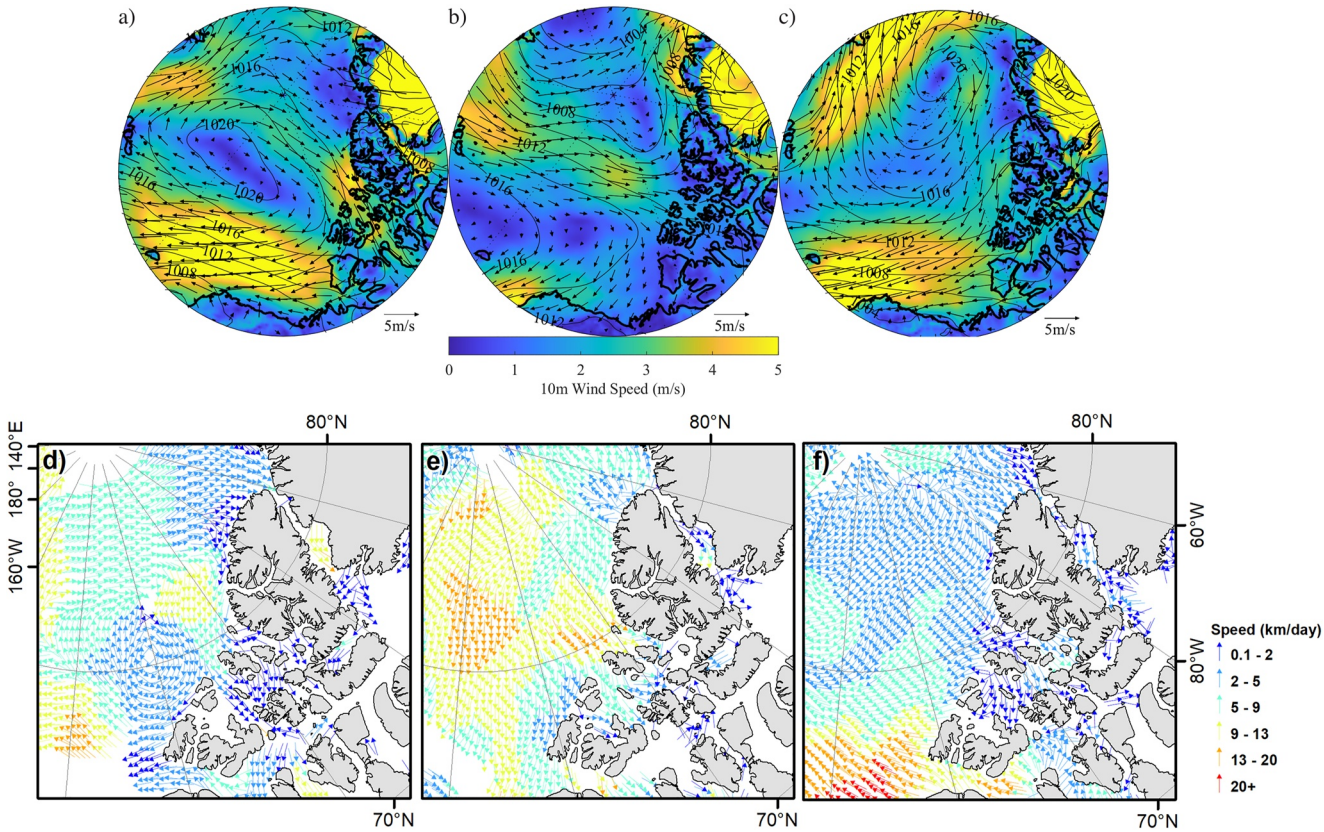

Figure 7. Monthly mean sea-level pressure (mb-contours), 10 m winds (m/s-vectors) and 10 m wind speed (m/s-shading) for (a) October 2017, (b) September 2020, and (c) October 2021. Sea ice motion for (d) 4–10 October, 2017, (e) 4–10 September, 2020, and (f) 10–17 October, 2021.

5. Conclusions

Both the sea ice area and volume fluxes between the Arctic Ocean and Nares Strait and the CAA were directly compared from October 2016 to December 2021 using high-resolution satellite-based sea ice motion products. Nares Strait provided the largest average seasonal (October through September) ice area flux of $95 \pm 8 \times 10^3$ km^2 followed by the CAA regions of the Queen Elizabeth Islands (QEI) at $41 \pm 7 \times 10^3$ km^2 and M'Clure Strait at $2 \pm 8 \times 10^3$ km^2 with corresponding ice volume fluxes of 177 ± 15 km^3, 59 ± 10 km^3, and 8 ± 8 km^3,

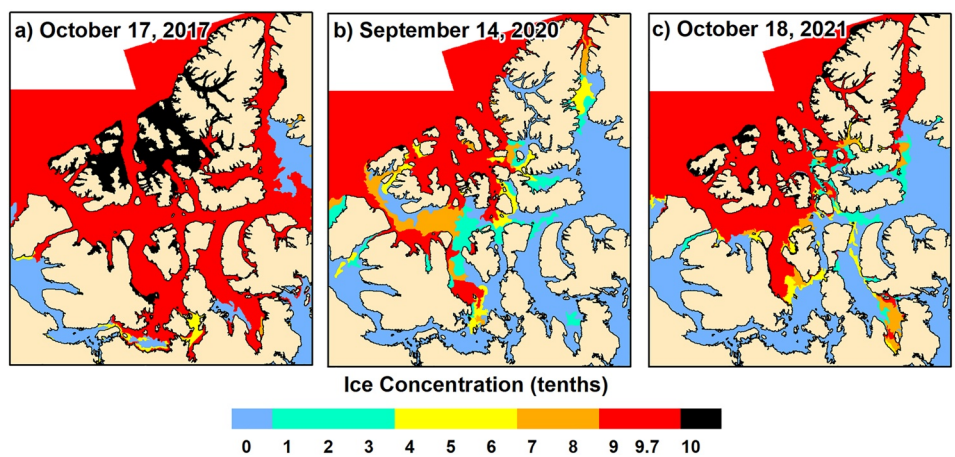

Figure 8. Ice conditions in the Canadian Arctic on (a) 17 October 2017, (b) 14 September 2020, and (c) 18 October 2021. Ice concentration of 10/10 (black) indicates landfast (immobile) sea ice.

21699291, 2023, 4, Downloaded from https://agupubs.onlinelibrary.wiley.com/doi/10.1029/2023JC019687 by Arctic University of Norway - UIT Tromso, Wiley Online Library on [17/07/2023]. See the Terms and Conditions (https://onlinelibrary.wiley.com/terms-and-conditions) on Wiley Online Library for rules of use; OA articles are governed by the applicable Creative Commons License

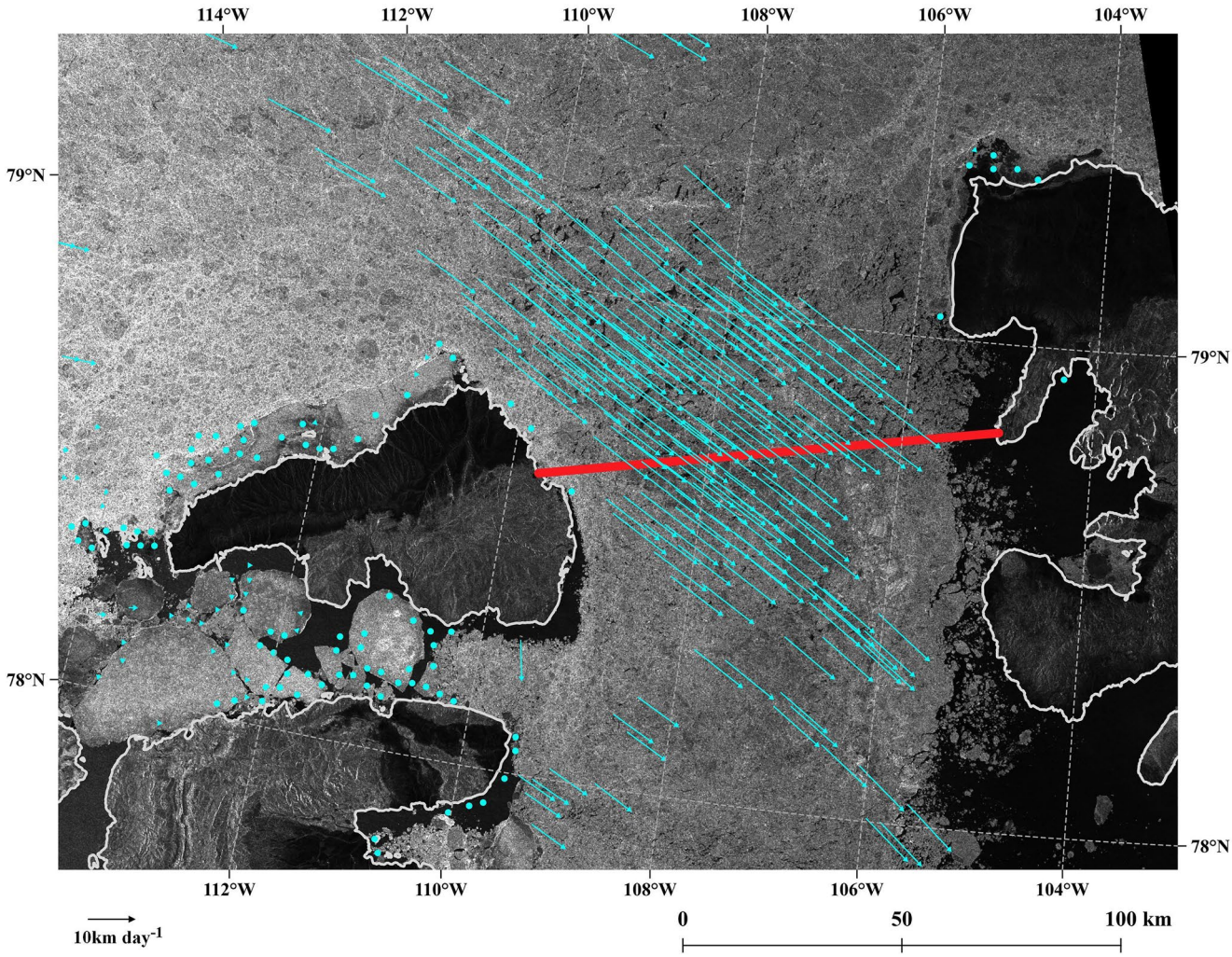

Figure 9. RADARSAT Constellation Mission (RCM) derived sea ice motion vectors (km/day) between 7 September 2020 and 8 September 2020 over the Prince Gustaf Adolf Sea region of the Queen Elizabeth Islands. The red line corresponds to the flux gate. Background is RCM image on 7 September 2020. (RCM © Government of Canada).

respectively. Larger and more variable Arctic Ocean ice export at Nares Strait was found to be associated with longer and more variable time periods between ice arch collapse and formation. This is compared to shorter and more consistent timing of ice arch formation and collapse for the QEI and M'Clure Strait regions.

On a net seasonal basis, the average Arctic Ocean ice area flux from all three gates was 138×10^3 km^2 and the volume flux was 245 km^3, which represents ~16% of the area and ~25% of the volume of sea ice export from Fram Strait. However, the dominant region for Arctic Ocean ice export was not always Nares Strait. Remarkably, the QEI was the dominant region for Arctic Ocean ice area export with 120×10^3 km^2 in 2020. Moreover, the September 2020 ice area flux value of 49×10^3 km^2 at the QEI was larger than any previous monthly value observed at Nares Strait from 1997 to 2009 (Kwok et al., 2010) and the time period of this study from October 2016 to December 2021. This is an important result and highlights the need to include the QEI in studies attempting to quantify the area (or volume) balance of sea ice in the Arctic Ocean. Moreover, considering the oscillating nature between Arctic Ocean ice import and export at M'Clure Strait it is also recommend to be included in area (or volume) balance estimates because it provides a potential source of Arctic Ocean ice replenishment or a sink for Arctic Ocean ice export.

There was considerable variability in the monthly ice flux values across all gates over the 5-year time period but there was no month when large Arctic Ocean ice export or import was coincident across all gates. Although large-scale atmospheric circulation can often affect several gates in a similar manner, the local ice conditions at

21699291, 2023, 4, Downloaded from https://agupubs.onlinelibrary.wiley.com/doi/10.1029/2023JC019687 by Arctic University of Norway - UIT Tromso, Wiley Online Library on [17/07/2023]. See the Terms and Conditions (https://onlinelibrary.wiley.com/terms-and-conditions) on Wiley Online Library for rules of use; OA articles are governed by the applicable Creative Commons License

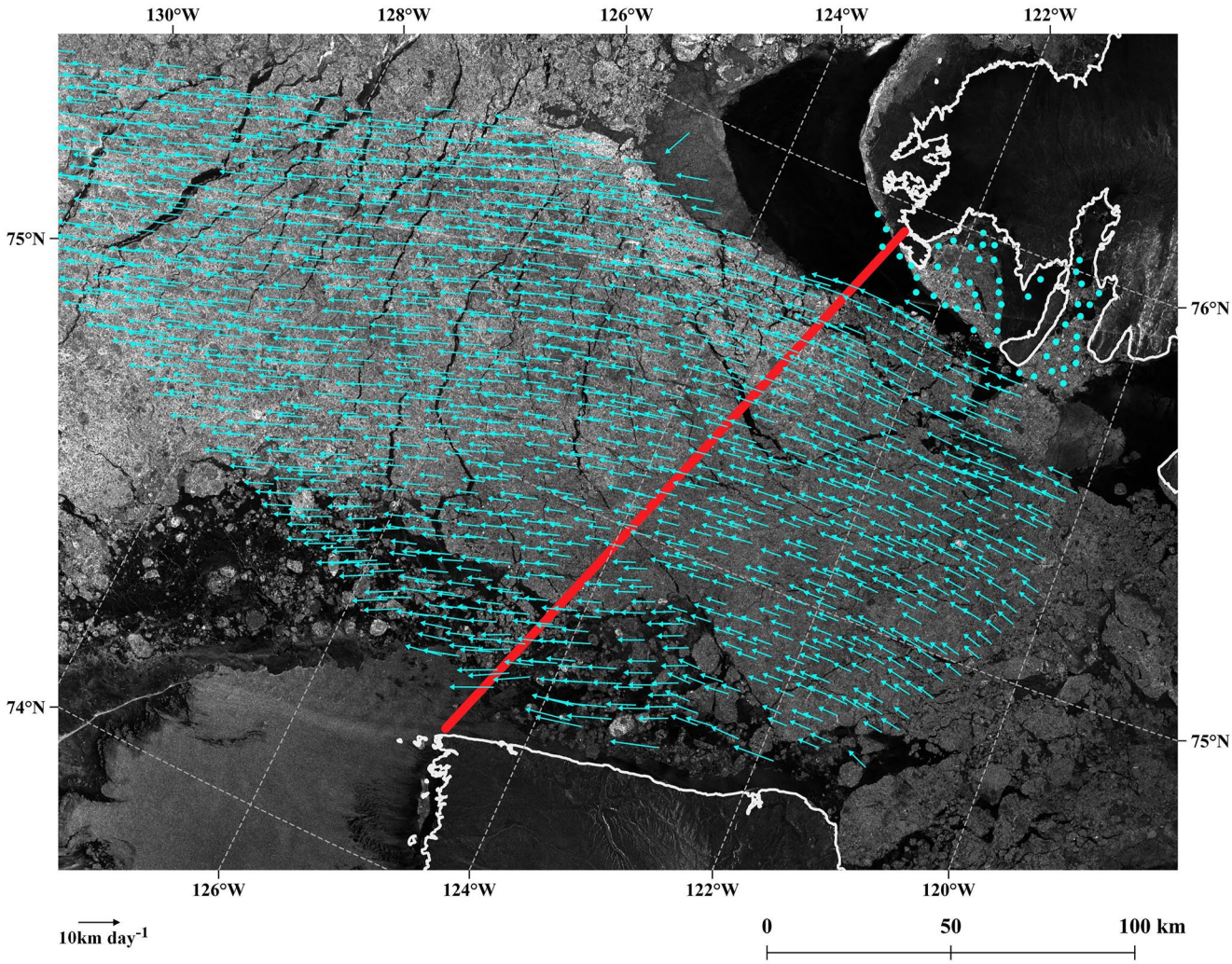

Figure 10. RADARSAT Constellation Mission (RCM) derived sea ice motion vectors (km/day) between 13 October 2021 and 14 October 2021 over M'Clure Strait. The red line corresponds to the flux gate. Background is RCM image on 13 October 2021. (RCM © Government of Canada).

each gate—through ice arch formation or buttressing by high ice concentrations—tend to reduce the covariance of fluxes between the three gates. This was the case in October 2017 when Arctic Ocean ice export through the QEI was limited by the presence of ice arches and a lack of open water within the CAA despite atmospheric forcing appearing to promote strong ice motion. In the absence of ice arches, together with available space (i.e., open water within pack ice), large-scale atmospheric circulation plays a dominant role in driving the Arctic Ocean ice area flux; but certain SLP patterns are more influential on certain gates than others. For instance, during September 2020 the QEI experienced large Arctic Ocean ice export while Nares Strait did not owing to the locations of high and low SLP, despite the fact both gates were open without arches.

Based on our ice flux observations from October 2016 to December 2021 it is unlikely these regions will experience large coherent Arctic Ocean ice export given the interplay between atmospheric circulation and ice conditions. As a result, it is more likely that Arctic Ocean ice export will gradually increase as ice arches persist for shorter and shorter durations as a result of Arctic warming, especially in Nares Strait and the QEI (Howell & Brady, 2019; Kwok et al., 2010; Moore et al., 2021; Ryan & Münchow, 2017). However, in recent years divergent Arctic Ocean export ice trajectories are apparent for Nares Strait and the QEI when compared to Fram Strait. As the Arctic sea ice retreats into the Last Ice Area during the summer months, the Arctic Ocean ice transport contributions from Nares Strait and the QEI could potentially surpass Fram Strait as the dominant pathway of Arctic Ocean ice export. M'Clure Strait is more variable and will continue to act as either a source or a sink of sea ice for the Arctic Ocean.

21699291, 2023, 4, Downloaded from https://agupubs.onlinelibrary.wiley.com/doi/10.1029/2023JC019687 by Arctic University of Norway - UIT Tromso, Wiley Online Library on [17/07/2023]. See the Terms and Conditions (https://onlinelibrary.wiley.com/terms-and-conditions) on Wiley Online Library for rules of use; OA articles are governed by the applicable Creative Commons License

Data Availability Statement

RADARSAT-2 and RADARSAT Constellation Mission (RCM) SAR imagery are available from Natural Resources Canada's Earth Observation Data Management System (https://www.eodms-sgdot.nrcan-rncan.gc.ca/index-en.html). Sentinel-1 SAR imagery are available from the Copernicus Open Access Hub (https://scihub.copernicus.eu/dhus/#/home). The Canadian Ice Service (CIS) digital ice charts are available from the CIS at: https://iceweb1.cis.ec.gc.ca/Archive/page1.xhtml?lang=en. Pan-Arctic large-scale sea ice motion from RCM and Sentinel-1 is available from Canada's Open Government Portal at: https://open.canada.ca/data/en/dataset/22aa3b41-425f-4f67-9747-f097c00e3eb1.

ERA5 monthly sea level pressure and wind speed is available from the Copernicus Climate Change Service (C3S) (2017). The year-round sea ice thickness observations from CryoSat-2 (Landy & Dawson, 2022) are available via the Polar Data Centre. The monthly sea ice area and volume flux values from October 2016 to December 2021(Howell et al., 2023) are available on Environment and Climate Change Canada's (ECCC) Open Data Server.

Acknowledgments

The authors dedicate this paper to the late Dr. Joshua King, who was a leader in radar remote sensing of snow.

D. Babb acknowledges support from the Natural Sciences and Engineering Research Council of Canada (NSERC) and is supported by the Canada Research Chair Program (D. Barber) and Canada Excellence Research Chair Program (D. Dahl-Jensen). J. Landy was supported by the European Space Agency project "EXPRO Polar + Snow on Sea Ice" under grant ESA AO/1-10061/19/I-EF and by the Research Council of Norway (RCN) projects CIRFA under Grant 237906 and INTERAAC under Grant 328957. G.W.K. Moore acknowledges support from the Natural Sciences and Engineering Research Council of Canada (NSERC).

References

Agnew, T., Lambe, A., & Long, D. (2008). Estimating sea ice area flux across the Canadian Arctic Archipelago using enhanced AMSR-E. *Journal of Geophysical Research*, *113*(C10), C10011. https://doi.org/10.1029/2007JC004582

Alt, B., Wilson, K., & Carrieres, T. (2006). A case study of old ice import and export through the Peary and Sverdrup Channels of the Canadian Arctic Archipelago. *Annals of Glaciology*, *44*, 329–338. https://doi.org/10.3189/172756406781811321

Babb, D. G., Galley, R. J., Asplin, M. G., Lukovich, J. V., & Barber, D. G. (2013). Multiyear sea ice export through the Bering Strait during winter 2011–2012. *Journal of Geophysical Research: Oceans*, *118*(10), 5489–5503. https://doi.org/10.1002/jgrc.20383

Babb, D. G., Galley, R. J., Howell, S. E. L., Landy, J. C., Stroeve, J. C., & Barber, D. G. (2022). Increasing multiyear sea ice loss in the Beaufort Sea: A new export pathway for the diminishing multiyear ice cover of the Arctic Ocean. *Geophysical Research Letters*, *49*(9), e2021GL097595. https://doi.org/10.1029/2021GL097595

Barber, D. G., Babb, D. G., Ehn, J. K., Chan, W., Matthes, L., Dalman, L. A., et al. (2018). Increasing mobility of high Arctic Sea ice increases marine hazards off the East Coast of Newfoundland. *Geophysical Research Letters*, *45*(5), 2370–2379. https://doi.org/10.1002/2017gl076587

Barber, D. G., Hanesiak, J. M., Chan, W., & Piwowar, J. (2001). Sea-ice and meteorological conditions in northern Baffin Bay and the North water polynya between 1979 and 1996. *Atmosphere-Ocean*, *39*(3), 343–359. https://doi.org/10.1080/07055900.2001.9649685

Canadian Ice Service. (2021). Sea ice climate normals for the northern Canadian waters 1991–2020. Retrieved from: https://www.canada.ca/en/environment-climate-change/services/ice-forecasts-observations/latest-conditions/climatology/ice-climate-normals/northern-canadian-waters.html

Copernicus Climate Change Service (C3S). (2017). ERA5: Fifth generation of ECMWF atmospheric reanalyses of the global climate. Copernicus Climate Change Service Climate Data Store (CDS). [Dataset] Retrieved from https://cds.climate.copernicus.eu/cdsapp#!/home

Dawson, G., Landy, J., Tsamados, M., Komarov, A. S., Howell, S., Heorton, H., & Krumpen, T. (2022). A 10-year record of Arctic summer sea ice freeboard from CryoSat-2. *Remote Sensing of Environment*, *268*, 112744. https://doi.org/10.1016/j.rse.2021.112744

Durner, G. M., Douglas, D. C., Nielson, R. M., Amstrup, S. C., McDonald, T. C., Stirling, I., et al. (2009). Predicting 21st century polar bear habitat distribution from global climate models. *Ecological Monographs*, *79*(1), 25–58. https://doi.org/10.1890/07-2089.1

Haas, C., & Howell, S. E. L. (2015). Ice thickness in the Northwest passage. *Geophysical Research Letters*, *42*(18), 7673–7680. https://doi.org/10.1002/2015GL065704

Hamilton, S. J., Castro de la Guardia, L., Derocher, A. E., Sahanathien, V., Tremblay, L. B., & Huard, D. (2014). Projected polar bear sea ice habitat in the Canadian Arctic Archipelago. *PLoS One*, *9*(11), e113746. https://doi.org/10.1371/journal.pone.0113746

Hibler, W. D., III, Hutchings, J. K., & Ip, C. F. (2006). Sea ice arching and multiple flow states of Arctic pack ice. *Annals of Glaciology*, *44*, 339–344. https://doi.org/10.3189/172756406781811448

Howell, S. E. L., Babb, D. G., Landy, J. C., & Brady, M. (2022). Multi-year sea ice conditions in the Northwest Passage: 1968-2020. *Atmosphere-Ocean*, *1*, 15. https://doi.org/10.1080/07055900.2022.2136061

Howell, S. E. L., Babb, D. G., Landy, J. C., Moore, G. W. K., Montpetit, B., & Brady, M. (2023). Monthly sea ice area and volume flux values for Nares Strait, Queen Elizabeth Islands, and M'Clure Strait from October 2016 to December 2021. [Dataset] Environment and Climate Change Canada's (ECCC) Open Data Server. Retrieved from https://crd-data-donnees-rdc.ec.gc.ca/CPS/products/IceFlux

Howell, S. E. L., & Brady, M. (2019). The dynamic response of sea ice to warming in the Canadian Arctic Archipelago. *Geophysical Research Letters*, *46*(22), 13119–13125. https://doi.org/10.1029/2019gl085116

Howell, S. E. L., Brady, M., & Komarov, A. S. (2022). Generating large-scale sea ice motion from Sentinel-1 and the RADARSAT constellation mission using the environment and climate change Canada automated sea ice tracking system. *The Cryosphere*, *16*(3), 1125–1139. https://doi.org/10.5194/tc-16-1125-2022

Howell, S. E. L., Wohlleben, T., Dabboor, M., Derksen, C., Komarov, A., & Pizzolato, L. (2013). Recent changes in the exchange of sea ice between the Arctic Ocean and the Canadian Arctic Archipelago. *Journal of Geophysical Research: Oceans*, *118*(7), 1–13. https://doi.org/10.1002/jgrc.20265

Howell, S. E. L., Wohlleben, T., Komarov, A., Pizzolato, L., & Derksen, C. (2013). Recent extreme light sea ice years in the Canadian Arctic Archipelago: 2011 and 2012 eclipse 1998 and 2007. *The Cryosphere*, *7*(6), 1753–1768. https://doi.org/10.5194/tc-7-1753-2013

Jeffers, S., Agnew, T. A., Alt, B. T., De Abreu, R., & McCourt, S. (2001). Investigating the anomalous sea-ice conditions in the Canadian high Arctic (Queen Elizabeth Islands) during summer 1998. *Annals of Glaciology*, *33*, 507–512. https://doi.org/10.3189/172756401781818761

Kirillov, S., Babb, D. G., Komarov, A. S., Dmitrenko, I., Ehn, J. K., Worden, E., et al. (2021). On the physical settings of ice bridge formation in Nares Strait. *Journal of Geophysical Research: Oceans*, *126*(8), e2021JC017331. https://doi.org/10.1029/2021JC017331

Komarov, A. S., & Barber, D. G. (2014). Sea ice motion tracking from sequential dual-polarization RADARSAT-2 images. *IEEE Transactions on Geoscience and Remote Sensing*, *52*(1), 121–136. https://doi.org/10.1109/TGRS.2012.2236845

Kwok, R. (2004). Annual cycles of multiyear sea ice coverage of the Arctic Ocean: 1999–2003. *Journal of Geophysical Research*, *109*(C11), C11004. https://doi.org/10.1029/2003JC002238

Kwok, R. (2005). Variability of Nares Strait ice flux. *Geophysical Research Letters*, *32*(24), L24502. https://doi.org/10.1029/2005GL024768

21699291, 2023, 4, Downloaded from https://agupubs.onlinelibrary.wiley.com/doi/10.1029/2023JC019687 by Arctic University of Norway - UIT Tromso, Wiley Online Library on [17/07/2023]. See the Terms and Conditions (https://onlinelibrary.wiley.com/terms-and-conditions) on Wiley Online Library for rules of use; OA articles are governed by the applicable Creative Commons License

Kwok, R. (2006). Exchange of sea ice between the Arctic Ocean and the Canadian Arctic Archipelago. *Geophysical Research Letters*, *33*(16), L16501. https://doi.org/10.1029/2006GL027094
Kwok, R. (2009). Outflow of Arctic Ocean sea ice into the Greenland and Barents seas: 1979–2007. *Journal of Climate*, *22*(9), 2438–2457. https://doi.org/10.1175/2008JCLI2819.1JClim
Kwok, R., & Cunningham, G. F. (2010). Contribution of melt in the Beaufort Sea to the decline in Arctic multiyear sea ice coverage: 1993–2009. *Geophysical Research Letters*, *37*(20), L20501. https://doi.org/10.1029/2010GL044678
Kwok, R., & Rothrock, D. A. (1999). Variability of Fram Strait flux and north Atlantic oscillation. *Journal of Geophysical Research*, *104*(C3), 5177–5189. https://doi.org/10.1029/1998jc900103
Kwok, R., Schweiger, A., Rothrock, D. A., Pang, S., & Kottmeier, C. (1998). Sea ice motion from satellite passive microwave data assessed with ERS SAR and buoy data. *Journal of Geophysical Research*, *103*(C4), 8191–8214. https://doi.org/10.1029/97jc03334
Kwok, R., Toudal Pedersen, L., Gudmandsen, P., & Pang, S. S. (2010). Large sea ice outflow into the Nares Strait in 2007. *Geophysical Research Letters*, *37*(3), L03502. https://doi.org/10.1029/2009GL041872
Landy, J., & Dawson, G. (2022). Year-round Arctic sea ice thickness from CryoSat-2 Baseline-D Level1b observations 2010-2020 (version 1.0) [Dataset]. NERC EDS UK Polar Data Centre. https://doi.org/10.5285/d8c66670-57ad-44fc-8fef-942a46734ecb
Landy, J., Dawson, G. J., Tsamados, M., Bushuk, M., Stroeve, J. C., Howell, S. E. L., et al. (2022). A year-round satellite sea ice thickness record from CryoSat-2. *Nature*, *609*(7927), 517–522. https://doi.org/10.1038/s41586-022-05058-5
Landy, J. C., Petty, A. A., Tsamados, M., & Stroeve, J. C. (2020). Sea ice roughness overlooked as a key source of uncertainty in CryoSat-2 ice freeboard retrievals. *Journal of Geophysical Research: Oceans*, *125*(5), e2019JC015820. https://doi.org/10.1029/2019jc015820
Lindsay, R. W., & Stern, H. L. (2003). The RADARSAT geophysical processor system: Quality of sea ice trajectory and deformation estimates. *Journal of Atmospheric and Oceanic Technology*, *20*(9), 1333–1347. https://doi.org/10.1175/1520-0426(2003)020<1333:TRGPSQ>2.0.CO;2
Maslanik, J., Stroeve, J., Fowler, C., & Emery, W. (2011). Distribution and trends in Arctic sea ice age through spring 2011. *Geophysical Research Letters*, *38*(13), L13502. https://doi.org/10.1029/2011GL047735
Melling, H. (2002). Sea ice of the northern Canadian Arctic Archipelago. *Journal of Geophysical Research*, *107*(C11), 3181. https://doi.org/10.1029/2001JC001102
Melling, H., Gratton, Y., & Ingram, G. (2001). Ocean circulation within the North water polynya of Baffin Bay. *Atmosphere-Ocean*, *39*(3), 301–325. https://doi.org/10.1080/07055900.2001.9649683
Moore, G. W. K., Howell, S. E. L., Brady, M., McNeil, K., & Xu, X. (2021). Anomalous collapses of Nares Strait ice arches leads to enhanced export of Arctic sea ice. *Nature Communications*, *12*, 1. https://doi.org/10.1038/s41467-020-20314-w
Moore, G. W. K., & McNeil, K. (2018). The early collapse of the 2017 Lincoln Sea ice arch in response to anomalous sea ice and wind forcing. *Geophysical Research Letters*, *45*(16), 8343–8351. https://doi.org/10.1029/2018GL078428
Moore, G. W. K., Schweiger, A., Zhang, J., & Steele, M. (2019). Spatiotemporal variability of sea ice in the Arctic's last ice area. *Geophysical Research Letters*, *46*(20), 11237–11243. https://doi.org/10.1029/2019GL083722
Newton, R., Pfirman, S., Tremblay, L. B., & DeRepentigny, P. (2021). Defining the "ice shed" of the Arctic Ocean's last ice area and its future evolution. *Earth's Future*, *9*, e2021EF001988. https://doi.org/10.1029/2021EF001988
Parkinson, C. L., & DiGirolamo, N. E. (2021). Sea ice extents continue to set new records: Arctic, Antarctic, and global results. *Remote Sensing of Environment*, *267*, 112753. https://doi.org/10.1016/j.rse.2021.112753
Perovich, D. K., Richter-Menge, J. A., Jones, K. F., & Light, B. (2008). Sunlight, water, and ice: Extreme Arctic sea ice melt during the summer of 2007. *Geophysical Research Letters*, *35*(11), L11501. https://doi.org/10.1029/2008GL034007
Ryan, P. A., & Münchow, A. (2017). Sea ice draft observations in Nares Strait from 2003 to 2012. *Journal of Geophysical Research: Oceans*, *122*(4), 3057–3080. https://doi.org/10.1002/2016jc011966
Samelson, R. M., Agnew, T., Melling, H., & Münchow, A. (2006). Evidence for atmospheric control of sea-ice motion through Nares Strait. *Geophysical Research Letters*, *33*(2), L02506. https://doi.org/10.1029/2005GL025016
Serson, H. V. (1972). *Investigations of a plug of multiyear old sea ice in the mouth of Nansen Sound. (DREO Tech. Note 72-6)*. Department of National Defence, Canada. Defence Research Establishment Ottawa.
Smedsrud, L. H., Halvorsen, M. H., Stroeve, J. C., Zhang, R., & Kloster, K. (2017). Fram Strait sea ice export variability and September Arctic sea ice extent over the last 80 years. *The Cryosphere*, *11*(1), 65–79. https://doi.org/10.5194/tc-11-65-2017
Spreen, G., De Steur, L., Divine, D., Gerland, S., Hansen, E., & Kwok, R. (2020). Arctic sea ice volume export through Fram Strait from 1992 to 2014. *Journal of Geophysical Research: Oceans*, *125*(6), e2019JC016039. https://doi.org/10.1029/2019JC016039
Stroeve, J., Liston, G. E., Buzzard, S., Zhou, L., Mallett, R., Barrett, A., et al. (2020). A Lagrangian snow evolution system for sea ice applications (SnowModel-LG): Part II—Analyses. *Journal of Geophysical Research: Oceans*, *125*(10), e2019JC015900. https://doi.org/10.1029/2019jc015900
Sumata, H., De Steur, L., Gerland, S., Divine, D. V., & Pavlova, O. (2022). Unprecedented decline of Arctic sea ice outflow in 2018. *Nature Communications*, *13*(1), 1747. https://doi.org/10.1038/s41467-022-29470-7
Thorndike, A. S., & Colony, R. (1982). Sea ice motion in response to geostrophic winds. *Journal of Geophysical Research*, *87*(C8), 5845–5852. https://doi.org/10.1029/JC087iC08p05845
Tilling, R., Ridout, A., Shepherd, A., & Wingham, D. J. (2015). Increased Arctic sea ice volume after anomalously low melting in 2013. *Nature Geosci*, *8*, 643–646. https://doi.org/10.1038/ngeo2489
Tivy, A., Howell, S. E. L., Alt, B., McCourt, S., Chagnon, R., Crocker, G., et al. (2011). Trends and variability in summer sea ice cover in the Canadian Arctic based on the Canadian ice service digital archive, 1960–2008 and 1968–2008. *Journal of Geophysical Research*, *116*(C3), C03007. https://doi.org/10.1029/2009JC005855
Vincent, R. F. (2019). A study of the North water polynya ice arch using four decades of satellite data. *Scientific Reports*, *9*(1), 20278. https://doi.org/10.1038/s41598-019-56780-6
Zhang, J. L., & Rothrock, D. A. (2003). Modeling global sea ice with a thickness and enthalpy distribution model in generalized curvilinear coordinates. *Monthly Weather Review*, *131*(5), 845–861. https://doi.org/10.1175/1520-0493(2003)131<0845:MGSIWA>2.0.CO;2

21699291, 2023, 4, Downloaded from https://agupubs.onlinelibrary.wiley.com/doi/10.1029/2023JC019687 by Arctic University of Norway - UIT Tromso, Wiley Online Library on [17/07/2023]. See the Terms and Conditions (https://onlinelibrary.wiley.com/terms-and-conditions) on Wiley Online Library for rules of use; OA articles are governed by the applicable Creative Commons License